Ab-initio Crystal Structure Determination From X-ray Powder Diffraction Data

Alok K. Mukherjee

Abstract | A wide range of crystalline solids cannot be prepared as single crystals of suitable size and/or quality for structure analysis using conventional single-crystal X-ray diffraction techniques. In such circumstances, it is essential that structural information can be obtained from powder diffraction. This article highlights some recent developments in the field of ab-initio crystal structure determination from X-ray powder diffraction data. Relevant fundamental aspects of different steps of structure determination procedure from powder data are described with particular emphasis to the challenging structure solution stage. Examples from our recent work are given to illustrate the potential of X-ray powder diffraction methodologies in determining crystal structures of several metal-organic complexes, organic compounds and pharmaceutical materials using diffraction data collected on a laboratory powder diffractometer.

1. Introduction

X-ray diffraction is undoubtedly the most important and powerful technique for characterizing the structural properties of crystalline solids, and many important scientific advances during the 20th century, for example, from high temperature superconductors to fullerenes, from nano technology to macromolecular crystallography, have relied heavily on this technique. By far the majority of crystal structure analyses have been carried out by single-crystal diffraction techniques using laboratory X-ray or advanced synchrotron radiation sources. While emphasizing the power of single-crystal X-ray diffraction methods for solving crystal and molecular structures of small- and macromolecules, it is important to note that an intrinsic limitation of this technique is the requirement to prepare single crystals of appropriate size and/or quality, which are not always met for all compounds in the chosen crystal growth conditions and also within a reasonable time scale. Although the limits in terms of size and quality of crystals that can be studied by single-crystal X-ray analysis are continually being extended by the recent developments in instrumentation and software for data analysis, many crystalline materials which give rise to good quality powder diffraction data are not amenable to investigation by single-crystal diffraction techniques. In such circumstances, it is essential that the structural information can be determined from X-ray powder diffraction. Considerable progress in the scope and potential of techniques for ab-initio structure solution from laboratory X-ray powder data has been made in recent years[1–4]. The present article gives an overview of the problems and challenges associated with structure determination from X-ray powder diffraction data, while focusing on examples from our own recent contributions in this field. More detailed reviews covering all aspects of structure

Department of Physics, Jadavpur University, Kolkata 700032, India.
akm@juphys.ernet.in

Figure 1: Schematic diagram illustrating the different stages involved in structure determination from powder diffraction data.

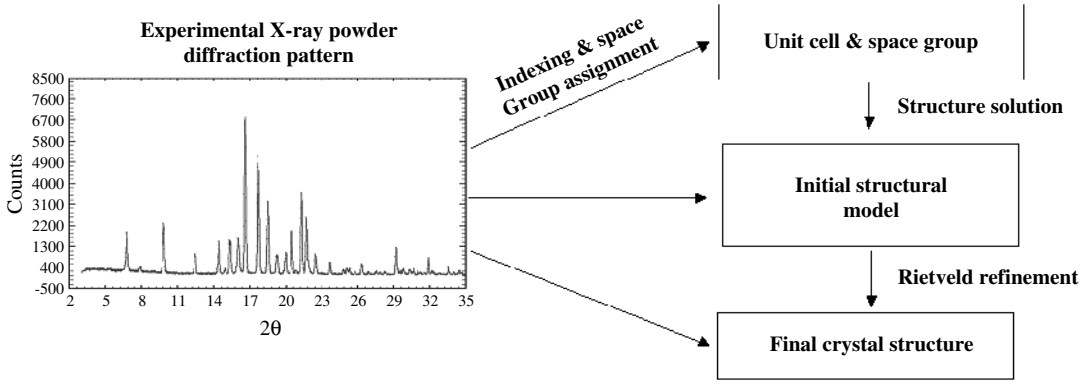

determination from powder diffraction data can be found elsewhere[5–7].

2. General aspects of structure determination from powder diffraction data

Crystal structure determination from powder diffraction data is generally divided into a series of steps, though there may be considerable overlap between different steps:

(i) Unit cell parameters determination (indexing)
(ii) Powder pattern decomposition
(iii) Space group assignment
(iv) Structure solution
(v) Structure refinement

Figure 2: Geometry of the Bragg-Brentano powder diffractometer with a conventional X-ray source (F) and incident-beam monochromator (M), short focal distance f_2 and focusing point F′. O is the diffractometer axis, D the detector and S_2 is the receiving slit. S_1 is an optional slit at F′.

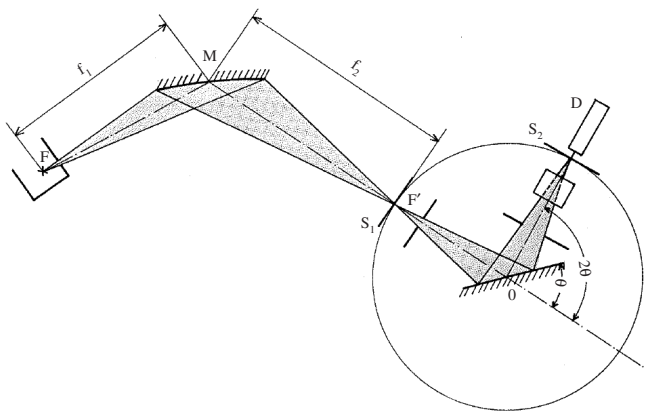

For determining the unit cell parameters, only peak positions in the observed diffraction pattern are needed, whereas the assignment of space group, structure solution, and structure refinement require consideration of relative intensities of different diffraction maxima. In the structure solution stage, the aim is to derive a starting model without any prior knowledge of arrangement of atoms, ions, or molecules in the unit cell. If the model is a good representation of the actual structure, an accurate crystal structure can be obtained by refining the structural model against the experimental powder diffraction data. The refinement of crystal structures using powder diffraction data can be carried out by the Rietveld refinement technique[8,9]. It is, however, important to recognize that ab-initio structure solution from powder diffraction data is still far from routine, and significant challenges must be overcome in developing and applying suitable methods for this purpose. A schematic overview of different stages of structure determination from powder diffraction data is shown in Fig. 1.

Although, single-crystal and powder-crystal X-ray diffraction patterns contain the same intrinsic information, in the former case this information is distributed in three- dimensional space, whereas in the latter case, the three-dimensional diffraction data collapse into the single dimension of a powder pattern. As a consequence, there is considerable overlap of peaks in a powder diffraction pattern. The overlapping of peaks in a powder pattern can be accidental or systematic. Non-equivalent reflections for which the peak positions (i.e. 2θ values) are sufficiently close to each other give rise to accidental overlapping and this is prevalent at high diffraction angles, and can be particularly severe for low symmetry structures, whereas well defined groups of nonequivalent reflections with identical

Figure 3: Summary of the steps involved in a Monte Carlo "move".

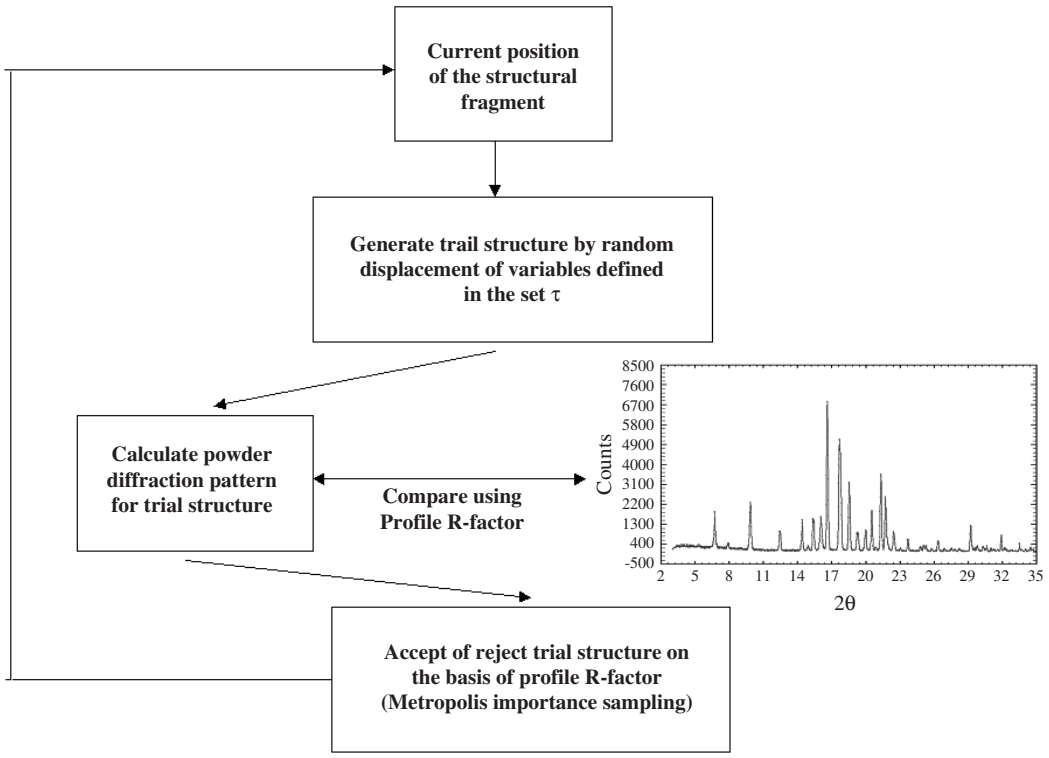

peak positions due to symmetry are responsible for systematic overlapping. The resulting ambiguity in powder diffraction data thus creates particular problems in determining the unit cell parameters and subsequent extraction of integrated intensities for a sufficiently large number of reflections. Indeed, all parts of structure solution process from powder diffraction data are less straightforward than their single-crystal counterparts.

3. Experimental considerations

A pre-requisite for crystal structure determination from powder diffraction is the availability of good quality data from the material to be investigated. Although, synchrotron X-ray powder diffraction data are clearly preferable due to substantially improved signal/noise ratio and higher resolution, the use of synchrotron data is generally not essential for solving moderately complex crystal structures. The majority of crystal structures determined till date using powder diffraction methodology have been obtained from conventional laboratory-based X-ray diffractometers. Modern in-house X-ray powder diffractometers with optimized optics offer sufficient resolution, precession and count rate to permit successful structure solution. The relative merits of different X-ray optics used for powder data collection have been discussed in several reviews[10,11].

Powder diffractometers operating in reflection and transmission geometries have now largely replaced earlier film cameras in most laboratories. Although, the reflection geometry using parafocusing Bragg-Brentano optics is most popular, the transmission geometry with thin films or capillary samples has some definite advantages for structure analyses and it requires only a small amount of sample. The instrument configuration most commonly used with conventional divergent-beam X-ray sources is based on Bragg-Brentano parafocusing geometry shown in Fig. 2. The source, sample, and receiving slit lie on the focusing circle, which has a radius dependent on angle θ. Coherently scattered X-rays from the flat sample then converge on a receiving slit placed in front of the detector. The detector rotates about the goniometer axis through twice the angular rotation of the sample ($\theta/2\theta$ scan). Although, the radiation most commonly used in conventional powder diffractometry is CuK$\alpha_{1,2}$ doublet, it is desirable to use monochromatic radiation in diffraction experiments operating in angle dispersive mode. Several advantages of using monochromatic radiation for ab-initio structure solution have been discussed by Louer

Figure 4: Final observed (crosses), calculated (red line), background (green line) and difference (blue line) profiles for $Pr(C_4H_4O_6)(C_4H_5O_6)(H_2O)$.

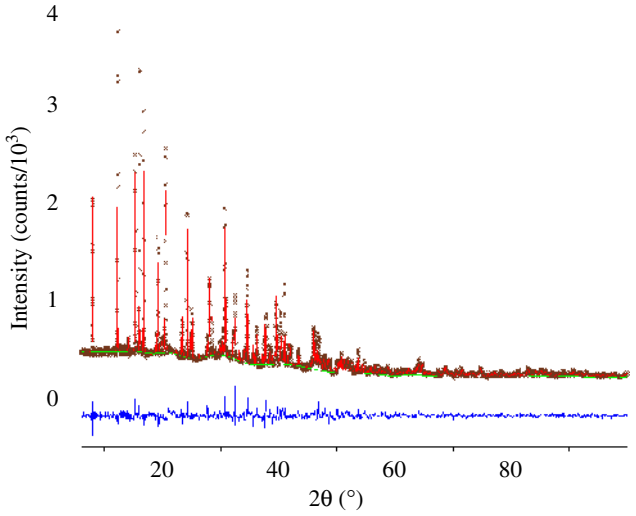

and Langford[12]. Significant improvement in the quality of powder diffraction data in terms of number of contributing reflections, full width half maxima (FWHM) of individual peaks, shape of the experimental profile and background counts can be achieved when monochromatic radiation (Kα1) is used instead of K$\alpha_{1,2}$ radiation.

4. Structure determination from powder diffraction data: The route map

4.1. *Powder pattern indexing*

The very first step in solving crystal structures from powder diffraction data involves determination of unit cell dimensions i.e. indexing the pattern. The complexity of indexing a powder pattern without any prior knowledge of either or both symmetry and dimensions of unit cell is inversely proportional to the symmetry of the lattice i.e. lower the symmetry, harder the indexing process. Clearly, it is not possible to proceed with structure solution and refinement unless the correct unit cell is found. The underlying physical principle of indexing a powder diffraction pattern is the reconstruction of a three-dimensional reciprocal lattice from a one-dimensional distribution of lengths d* of reciprocal-lattice vectors. The basic equation used for indexing a powder diffraction pattern is

$$1/d^2_{hkl}(Q_{hkl}) = h^2a^{*2} + k^2b^{*2} + l^2c^{*2} + 2klb^*c^*cos\alpha^* + 2hlc^*a^* \cos\beta^* + 2hka^*b^*\cos\gamma^* \quad (1)$$

where, d_{hkl} is the interplanar spacing corresponding to the (hkl) plane and $a*, b*, c*, \alpha*, \beta*, \gamma*$ are cell parameters of the reciprocal unit cell. The above equation expressed as a function of direct cell parameters is given in most textbooks on powder diffraction[13]. Considering an absolute error ΔQ_i in the observed peak position (normally achieved from a peak-search process), indexing of a powder pattern consists of finding the linear and angular parameters of the unit cell, from which a set of Miller indices, hkl, can be assigned to each observed line Q_{io}, within the experimental error, i.e.

$$Q_{io} - \Delta Q_i \leq Q_{ic} \leq Q_{io} + \Delta Q_i \quad (2)$$

For accurate indexing of a powder diffraction pattern from first principle the following four points play vital role.

(i) The availability of Bragg peaks observed at the lowest possible 2θ values is critically important because these peaks usually correspond to simple indices ($-2 \leq h \leq 2, -2 \leq k \leq 2, -2 \leq l \leq 2$). This considerably limits the possibilities of locating the corresponding vectors in reciprocal lattice and therefore simplifies the whole process of indexing.

(ii) Due to absence of a large number of extinct Bragg peaks, especially at low angles, all observed Bragg peaks taken into account during indexing might have one of the indices divisible by two. The resulting unit cell dimension will then become half of the true value.

(iii) Systematic errors in the experimental diffraction data due to sample displacement and/or zero shift errors may considerably influence the outcome of indexing process, because only the lengths but not the directions of reciprocal lattice vectors are measurable in powder diffraction experiments.

(iv) The presence of Bragg peaks due to an impurity phase (or a second polymorph of the material of interest) in the experimental data often constitutes an intractable problem for ab-initio indexing (unless the presence of the impurity phase (s) is known in advance). If a solution is ever found, it is unlikely to be correct as it describes both vectors from the major phase and the impurity phase (s) in the same reciprocal lattice.

The main approaches for automatic indexing of a powder diffraction pattern are based on the zone indexing principle[14], index permutation procedure[15] and successive dichotomy method[16].

Figure 5: (a) Molecular packing of $[Pr(C_4H_4O_6)(C_4H_5O_6)(H_2O)]$ viewed along [001] direction. (b) Tetranuclear $Pr_4C_{10}O_8$ motif having 7.59 Å × 6.94 Å dimension. (c) Formation of helical chains along the a-axis. (d) Linking of successive Pr coordination polyhedron along the c-axis.

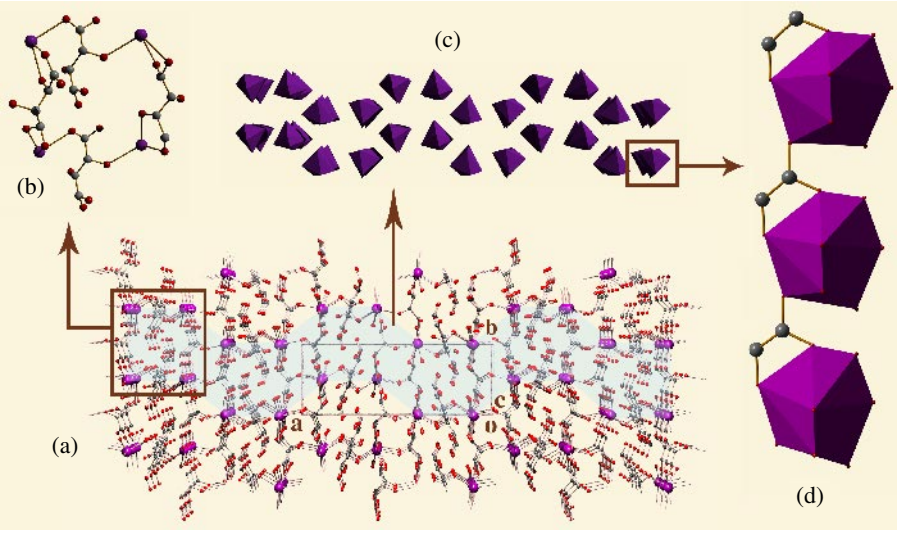

The most widely used computer programs for ab-initio indexing are ITO[17], TREOR[15], DICVOL[18] and CRYSFIRE[19]. The necessary input for these auto-indexing programs is normally the measured 2θ positions of peak maxima for a number (about 20) of selected peaks. Since different auto-indexing programs adopt different approaches as mentioned earlier, it is advisable to use more than one programs to check the reproducibility of indexing. Our experience shows that relative success of different auto-indexing programs can differ from one set of powder diffraction data to another. A comparative study of powder pattern indexing with various programs has been reported by Neumann[20]. There has been relatively little fundamental development of powder indexing methods since the pioneering work several years ago. New indexing strategies based on whole-profile fitting and global optimization using genetic algorithm[21] and iterative use of singular value decomposition technique[22] has been developed recently[23]. For a comprehensive collection of different crystallographic software, readers are referred to the International Union of Crystallography website at http://www.iucr.org.

In general, auto-indexing programs generate several possible sets of lattice parameters that are consistent to a greater or lesser degree with a set of measured positions. Thus, regardless of how we index a powder diffraction pattern, we need some simple criteria to assess the reliability of indexing. P. M. de Wolff[24], who proposed several "figure of merits" (FOM) for this purpose. The de Wolff FOM (M_{20}) is defined as

$$M_{20} = \frac{Q_{20}}{2|\Delta Q|_{av}} \cdot \frac{1}{N_{20}} \qquad (3)$$

where, Q_{20} is the $Q(1/d^2_{hkl})$ value for the 20th observed line, N_{20} is the number of calculated Q values upto Q_{20}, and $|\Delta Q|_{av}$ is the average absolute discrepancy between the observed and calculated Q_{hkl} for the first 20 Bragg peaks. Another figure of merit F_N, has been proposed by Smith and Snyder[25],

$$F_N = \frac{1}{|\Delta 2\theta|_{av}} \cdot \frac{N_{obs}}{N_{poss}} \qquad (4)$$

where, N_{poss} is the number of calculated diffraction lines up to the Nth observed line and $|\Delta 2\theta|_{av}$ is the average absolute discrepancy between the observed and calculated 2θ values. From a consideration of respective merits of M_{20} and F_N[26,27], it was pointed out that F_N is more appropriate for evaluating the quality of a powder diffraction data set whereas M_{20} is preferable for indexing purpose. Higher the accuracy of data collection and more complete the observed diffraction pattern, the larger will be M_{20} and F_N values. As a thumb rule, the M_{20} FOM should not be lower than 10 in order to accept a solution with confidence. Although it is impossible to make a rigorous test of the reliability of powder indexing, larger M_{20} (>20) and F_n (>40) values give higher probabilities of correctness of the solution.

Figure 6: The Rietveld refinement plot for $[\{VO_2(C_{12}H_{17}N_2O)\}_2]$. Final observed (crosses), calculated (red line), background (green line) and difference (blue line).

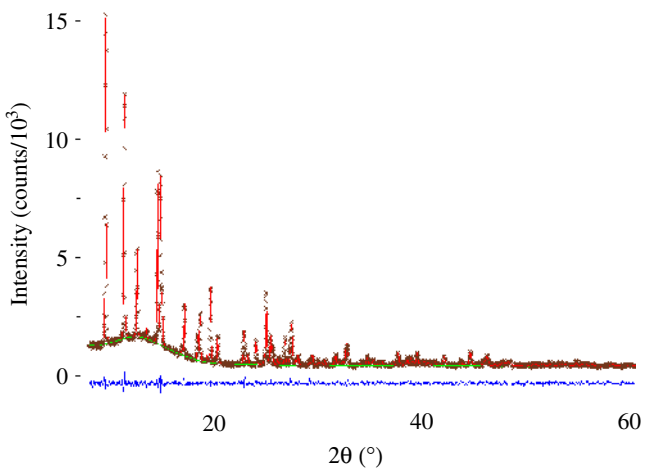

Figure 7: The molecular view of $[(VO_2)_2(C_{12}H_{17}N_2O)_2]$ with atom numbering scheme. Symmetry code: (i) 1-x, 2-y, -z.

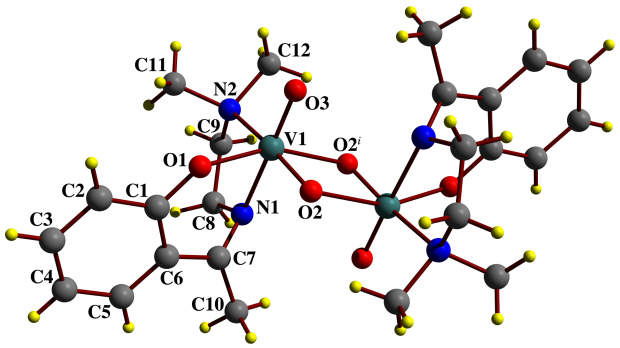

4.2. *Extraction of integrated intensities*

The main obstacle in ab-initio structure solution from X-ray powder diffraction data using single-crystal like approaches is the lack of accuracy of extracted intensities of Bragg reflections. Considerable efforts have been devoted in the past thirty years for estimating reliable integrated intensities from powder pattern decomposition[28,29]. In the whole powder pattern decomposition techniques, a calculated pattern is fitted to the entire observed profile by minimizing a function residual S

$$S = \sum_{i=1}^{N} \omega_i(2\theta)\{y(2\theta_i)_{obs} - y(2\theta_i)_{cal}\}^2 \qquad (5)$$

where, $y(2\theta_i)_{obs}$ and $y(2\theta_i)_{cal}$ are the observed and calculated intensities at the ith step of the digitized powder pattern, $\omega_i(2\theta)$is the appropriate weighting factor, and the summation running over all data points. The calculated intensity, $y(2\theta_i)$, can be expressed as

$$y(2\theta_i)_{cal} = b(2\theta_i) + \sum_j I_j P(2\theta_i)_j \qquad (6)$$

where, $b(2\theta_i)$ is the background intensity, I_j is the integrated intensity corresponding to the j^{th} reflection, $P(2\theta_i)$ is the profile function used to model the experimental peak, and summation is over all reflections which contribute to the intensity at $2\theta_i$. The agreement between the observed and calculated profiles can be assessed using several criteria. The most commonly used indicator is weighted profile R-factor (residual factor), R_{wp}, which is defined as

$$R_{wp} = 100 \times \left[\frac{\sum_{i=1}^{N} \omega_i\{y(2\theta_i)_{obs} - y(2\theta_i)_{cal}\}^2}{\sum_{i=1}^{N} \{\omega_i(2\theta_i)_{obs}\}^2} \right]^{1/2} \qquad (7)$$

Two approaches, the Pawley method[30] and Le Bail method[31], are widely followed for decomposition of X-ray powder profile. In the Pawley method, which minimizes the sum of squares of differences between the observed and calculated profiles, the set of parameters refined in the least-squares process include the integrated intensities, the cell dimensions and the parameters for modeling the background and peak shape. Since the method is based on a non-linear least-squares procedure, it may end up with unreliable negative integrated intensity values due to high correlation between the diffraction intensities. Special techniques based on Bayesian analysis have been developed[32,33] to reduce the intensity correlation and provide positive integrated intensity values.

The Le Bail method is an iterative process based on the Rietveld decomposition formula[8], in which the observed intensity is partitioned according to the calculated intensity. It is computationally efficient, does not require least-squares matrix inversion, and thus provides positive integrated intensity values. The main drawback of this algorithm is that it assigns equal intensities to completely overlapping reflections. To overcome the problem of equipartitioning of intensities in the Le Bail algorithm, several modifications have been proposed[34–36]. Monte Carlo methods have also been applied recently to provide different partitions of intensities of overlapping reflection cluster[29]. A number of programs including ALLHKL[37], WPPF[38], GSAS[39], FULLPROF[40], PROFIL[41] and EXPO[42] are available for powder pattern decomposition.

Figure 8: Hexanuclear supramolecular motif of $[\{VO_2(C_{12}H_{17}N_2O)\}_2]$, having 9.0 Å × 13.9 Å dimension.

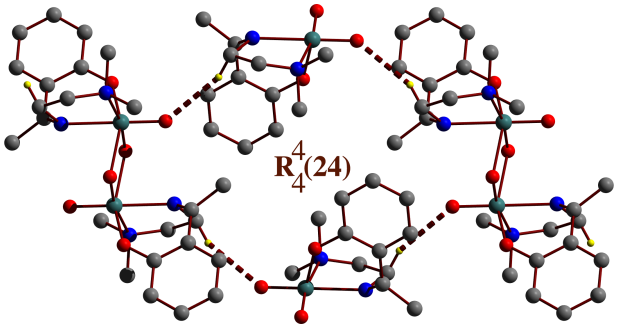

Figure 9: The molecular view of o-hydroxy acetophenone, $(C_{10}H_{12}O_3)$, (I) with atom numbering scheme.

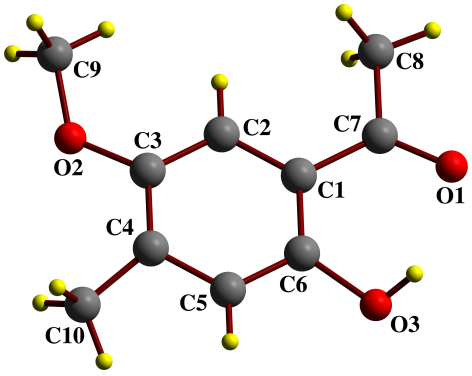

4.3. *Space group assignment*

In the structure solution pathway from powder diffraction data, determination of space group is a critical step. After successful indexing and pattern decomposition, the space group can be assigned by a careful investigation of systematic absences in the intensity data. If it is not possible to assign the space group uniquely, structure solution should be attempted separately for each of the plausible space groups. The determination of unit cell volume, space group and density can establish the contents of the crystallographic asymmetric unit. Supplementary information from other experiments (particularly solid state NMR) may be helpful in confirming the number of molecules and/or structural units in the asymmetric unit.

Following the Bayesian probabilistic approach, a novel method avoiding the manual inspection of diffraction intensities was developed by Markvardsen et al.,[43] which estimates the relative probabilities of different extinction symbols. Experimental powder diffraction pattern once indexed and decomposed into single diffraction intensities, is subjected to statistical analysis to calculate the probability values for different extinction symbols compatible with the crystal system under investigation. The most probable extinction symbol usually corresponds to the correct one, although the discrimination in terms of probabilities corresponding to the correct and incorrect groups is not always significant. Once the extinction symbol has been established, the choice of space group is not difficult. The algorithm for space group determination via probabilistic approach has been implemented in EXPO-2004[42] and its upgraded version EXPO-2006[44].

4.4. *Structure solution methodology*

Structure solution from X-ray powder diffraction is, generally, the most difficult and challenging part among the various stages outlined in section 2. Various advances in terms of development of novel methodologies and improved instrumentation have been made in the field of ab-initio structure determination from powder diffraction. The present section gives an overview of techniques that are currently available for structure solution using X-ray powder diffraction data. These techniques can be broadly classified into two categories: traditional and direct space approaches.

4.4.1. *Traditional approaches*

In the traditional or reciprocal-space based methods (i.e. Patterson and direct methods) for solving crystal structures from powder data, intensities of individual reflections are extracted directly from the experimental powder pattern and then used as input for structure solution techniques developed for single crystal diffraction data. Patterson or direct methods give results of less reliability particularly when strongly affected by peak overlap in a powder diffraction pattern, which in turn limits the reliability of the extracted intensities and can therefore lead to considerable difficulty in subsequent efforts to solve the structure using these intensity data. For molecular crystals with large unit cell volume, low symmetry and more that one molecules in the asymmetric unit, structure solution attempts from powder diffraction data using traditional approaches are unlikely to be successful. Despite these intrinsic difficulties, there have been successes in the application of traditional methods for structure solution from powder diffraction data. Since Patterson method is able to derive an approximate structural model from powder diffraction data that are somewhat inferior in quality, it can be applied for structure solution

Figure 10: Rietveld plot for $C_{10}H_{12}O_3$ (I) showing observed data (black curves), calculated profile (red curve), difference curve (blue curve) and calculated background (green line).

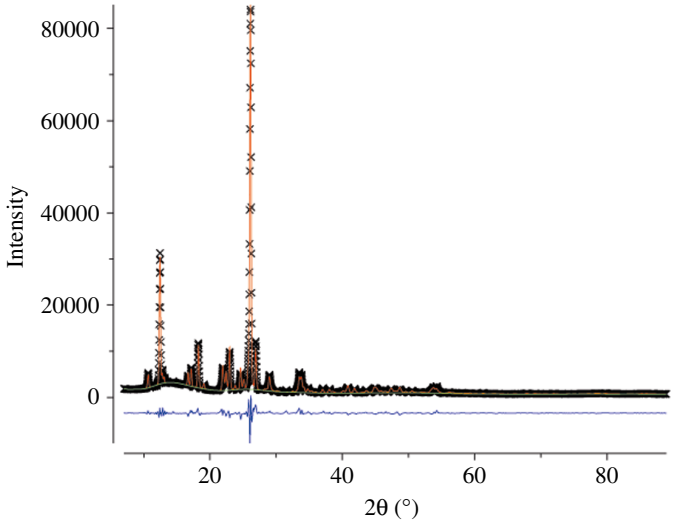

Figure 11: The molecular view of o-hydroxy acetophenone, ($C_{13}H_{18}O_3$), (II) with atom numbering scheme.

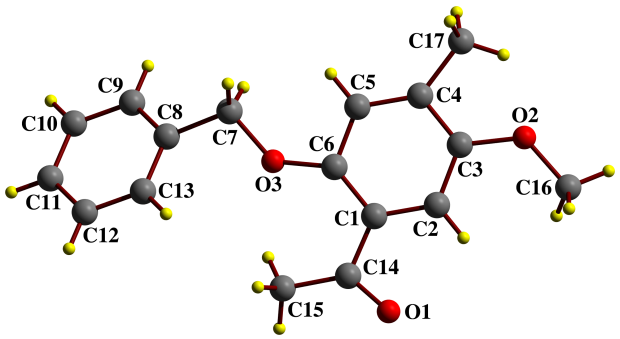

provided the structure contains a small number of dominant scatterers or a structural fragment of well-defined geometry[45–47].

Although direct methods as implemented in different program packages, for example, MULTAN[48], SHELXS[49], SIR[50], SIMPEL[51] have been routinely used for solving crystal structures of small molecules (say upto 200 non-hydrogen atoms in the asymmetric unit) using single crystal X-ray diffraction data, their application to small organic crystal structures is often unsuccessful when only powder diffraction data are available. The apparent reason for this is the availability of less number of triplet invariants with high Cochran reliability factor[52] and thereby weakening the phasing process, and the inaccuracy of integrated intensities extracted for different reflections from the experimental powder diffraction pattern following Pawley or Le Bail approach described earlier (see section 4.2). A steady stream of new developments[42,44] and their incorporation in the program package EXPO now allow successful application of direct methods for solving crystal structures from powder diffraction data[53]. Other techniques, for example, the maximum entropy and likelihood method that follows a similar approach to conventional direct methods have also been applied to solve crystal structures from powder diffraction data[54–57]. Considering an unknown crystal structure consisting of randomly distributed atoms in the asymmetric unit, the structure solution process aims at removing the randomness gradually. When applied to powder diffraction data, the maximum entropy and likelihood method automatically takes care groups of overlapping peaks in a powder pattern in a rational manner, and the intensity information for these peaks is used in the structure solution process. The maximum entropy and likelihood method optimized for powder diffraction data has been implemented in the program MICE[58].

4.4.2. *Direct-space approaches*

In view of the difficulties encountered while applying traditional methods for solving crystal structures of moderate complexity from powder diffraction data, alternative structure solution strategies, the so-called direct-space methods, have been developed. In the direct-space approaches[59,60], trial structures are generated in direct space, independently of experimental powder diffraction data, and the suitability of each trial structure is assessed by direct comparison between calculated powder diffraction pattern based on the trial structure and observed powder pattern. The comparison between the experimental and calculated powder profiles is usually monitored by the weighted powder profile R-factor, R_{wp}, defined in equation (7). As R_{wp} calculation considers the entire digitized powder data point-by-point rather than the integrated intensities of individual diffraction maxima, the peak overlap in powder pattern is implicitly taken into account. The direct-space strategies have been found to be particularly advantageous when some prior structural knowledge (i.e. types of rigid groups and connectivity among various groups) is available for the compound under study, since it can be actively used during the structure solution process. The first compound of unknown crystal structure to be solved from powder diffraction data using

Figure 12: Rietveld plot for $C_{13}H_{18}O_3$ (II) showing observed data (black curves), calculated profile (red curve), difference curve (blue curve) and calculated background (green line).

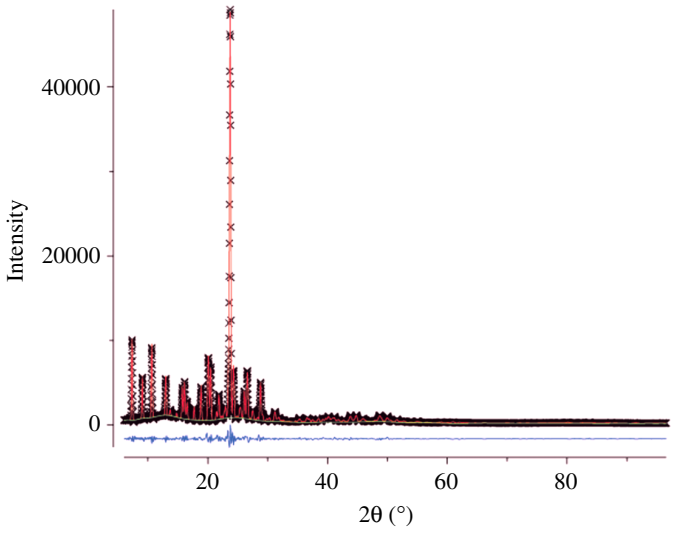

a direct-space approach was reported by Harris et al.[61]. The basis of all direct-space methods is a global optimization problem of great complexity in which the agreement between the calculated and observed diffraction patterns is maximized. This is equivalent to exploring a hypersurface by varying the structural variables in order to find it's global minimum. As a consequence, any global-optimization search algorithm may be used to find the global minimum, and several methods such as grid search[62,63], genetic algorithm[61], Monte Carlo and simulated annealing[64] have been embodied within the direct-space techniques for structure solution. Different computer programs using direct-space approaches are available, such as FOX[65], POWDER SOLVE[66], ESPOIR[67], TOPAS[68], EAGER[69], ENDEAVOUR[70], DASH[71], GAPSS[72] (for a full list see http://www.cristal.org/iniref.html).

Figure 13: Formation of C(6) chain in $C_{10}H_{12}O_3$(I).

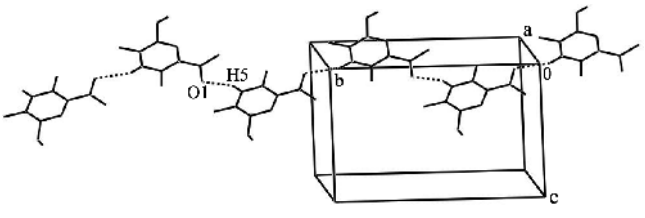

4.4.3. *Monte Carlo and Simulated Annealing techniques*

Of the different global optimization techniques for solving structures from powder diffraction data, the Monte Carlo/Simulated Annealing and Genetic Algorithm methods are most commonly used. The foundations of the Monte Carlo and simulated annealing methods are very closely related, and in both cases, a sequence of structures (T_i, where $i = 1, 2, \ldots N$) is generated for consideration as probable structure solutions. Each trial structure is defined by a set of structural variables, which include the position, orientation and intramolecular geometry of each molecule in the asymmetric unit. Starting from the structure T_j, a trial structure $T_{j,trial}$ is generated by making small random displacement to each of the structural variables in T_j. An appropriate figure of merit criteria, such as R_{wp}, is used to estimate the agreement between the powder diffraction pattern calculated for the trial structure and the experimental powder diffraction pattern. Considering the difference Z, where

$$Z = R_{wp}(T_{j,trial}) - R_{wp}(T_j) \qquad (8)$$

and invoking the Metropolis sampling algorithm, the trial structure is automatically accepted if $Z \leq 0$, whereas if $Z > 0$, the trial structure is accepted with a probability $\exp(-Z/S)$ and rejected with a probability $[1 - \exp(-Z/S)]$, where S is an appropriate scaling factor. After a sufficiently wide range of parameter space has been explored, the best solution (corresponding to lowest R_{wp}) is identified as the starting model structure for refinement. A workflow for each Monte Carlo move is shown in Fig. 3. The fundamental difference between the Monte Carlo and simulated annealing techniques is the way in which the parameter S is used to control the sampling algorithm. In the Monte Carlo method, S may be fixed or varied manually, whereas in the Simulated Annealing technique, S is decreased systematically according to an annealing schedule or temperature reduction procedure.

The efficiency of Monte Carlo method in solving structures from powder diffraction data depends on the number of structural degrees of freedom varied during calculation. The method seems to be more efficient for organic compounds and metal-organic complexes, where the structural fragments can be represented by rigid group of atoms in which only the position and orientation of the structural fragments are to be varied in the Monte Carlo calculation. Thus, for successful structure solution from powder diffraction data using Monte Carlo approach, the number of degree of freedom in the structural fragments is, in general, a more important consideration than the number of atoms in the asymmetric unit.

Figure 14: C-H...π stacking interaction in $C_{13}H_{18}O_3$(II).

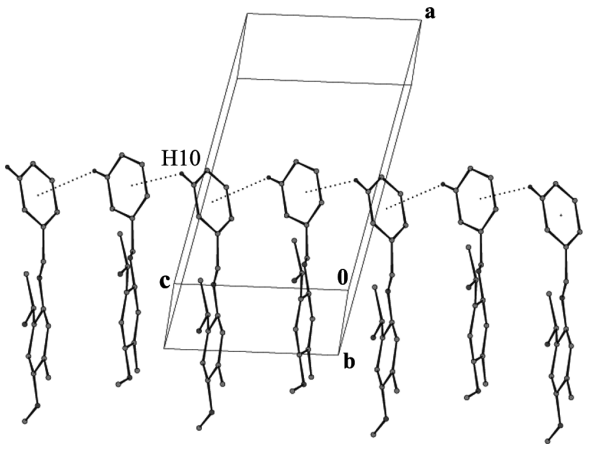

4.4.4. *Genetic Algorithm technique*

The genetic algorithm is a direct space optimization technique[73] based on the evolution principle of biological systems, in which only the members that fit best into environment survive. The improved subsequent generation is obtained from the current state of a system and events that are equivalent to mating, mutation and natural selection. The use of this technique in structure solution from X-ray powder diffraction data investigates the evolution of a population of trial crystal structures, with each member of a population defined by a set of variables T representing the coordinates (x, y, z) of the center of mass of molecule or a selected atom, the rotation angles (θ, ϕ, ψ) around three orthogonal axes, and torsion angles $(\tau_1, \tau_2, \ldots \tau_n)$ specifying the intramolecular geometry. Since each member of population is uniquely characterized by these variables, the set T is regarded as it's genetic code. The initial population P_0 comprising of N_p randomly generated structures is being allowed to evolve through subsequent generations by applying the evolutionary operations of mating, mutation and natural selection. These operations convert a particular generation (population P_j) to the next generation (population P_{j+1}). The number (N_p) of structures in the population remains constant for all generations, and N_m mating operations and N_x mutation operations are performed during evolution of a given population P_j to population P_{j+1}. The quality of each structure in the population is assessed by appropriate fitness function, which can be the weighted profile R-factor, R_{wp}, as defined earlier or the figure of merit, χ^2, based on the intensities of individual reflections extracted from the powder diffraction pattern [74,77]. The probability that a given structure survives into next generations, and the probability it takes part in mating, depend on it's fitness. In the natural selection process, only the best structures with highest fitness are allowed to pass from one generation to next generation during genetic algorithm calculation. After the population has evolved for a sufficient number of generations, the member of the population (i.e. the structure) with highest fitness should be close to the correct structure.

In contrast to other approaches for global optimization, the genetic algorithm technique involves simultaneous sampling of different regions of parameter space, and the information from different regions of parameter space is passed actively between different members of the population by mating operations. Thus the genetic algorithm technique operates in a parallel rather than a sequential manner and can be readily beneficial for parallel computing strategies.

4.5. *Rietveld refinement*

The final stage in structure determination procedure from X-ray powder diffraction data (as outlined in section 2), the structure refinement, is generally carried out by the Rietveld method[8] which considers every point in the digitized powder diffraction profile as an individual intensity measurement. The history, theory and practice of structure refinement with powder diffraction data using Rietveld method can be found in a number of text books and review articles[4,9]. In the Rietveld refinement of a crystal structure using powder diffraction data, the variables defining the structural model (atomic positions and atomic displacement parameters) and the powder diffraction profile (unit cell parameters and zero shift error, analytical functions describing the peak shape and peak width, background intensity coefficients) are adjusted by least-squares methods so that an optimal fit between the experimental and calculated powder diffraction patterns is achieved. The peak shape in a X-ray powder diffraction pattern depends on the characteristic properties of both instrument and sample, and the most widely used peak shape function for X-ray powder diffraction data is pseudo-Voigt function, which represents a hybrid of Gaussian and Lorentzian characters of peak shape. Several criteria for assessing the agreement between experimental and calculated powder diffraction patterns can be used[4,9]. Some commonly used programs for Rietveld refinement are GSAS[39], FULLPROF[40], PROFIT [41] and RIETAN [76].

For successful Rietveld refinement, the initial model structure obtained in structure solution

Figure 15: Rietveld plot for piroxicam metoxybenzoate ($C_{23}H_{19}N_3O_6S$) showing observed data (black curves), calculated profile (red curve), difference curve (blue curve) and calculated background (green line).

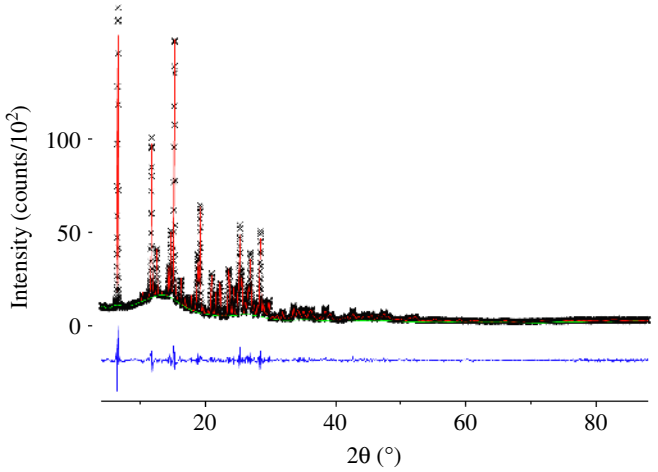

stage must be a good representation of the correct structure. It is generally necessary to use geometric restraints based on standard molecular geometries to avoid problems of instability during Rietveld refinement and to achieve stable convergence of least-squares calculation.

5. Examples of structure determination using laboratory X-ray powder diffraction data

The present section highlights some of the crystal structures that have been determined by our group in recent years using laboratory X-ray powder diffraction data. The examples are chosen from a range of fields, i.e. metal-organic complexes, organic compounds and pharmaceutical materials, to illustrate the potential of X-ray powder diffraction for ab-initio crystal structure determination. In each case, powder diffraction data have been collected at ambient temperature on a conventional laboratory diffractometer operating in the Bragg-Brentano geometry with a primary beam germanium monochromator ($CuK_{\alpha 1}$ radiation).

5.1. *A novel praseodymium tartrate*

Structural understanding of lanthanide tartrates is of fundamental importance due to variable and high coordination numbers of trivalent lanthanide ions, and conformational flexibility of organic ligand with the ability to behave as completely or partially deprotonated. Since many lanthanide tartrates including praseodymium tartrate synthesized under hydrothermal condition are available only as microcrystalline powder, the structure analysis of the Pr compound, $[Pr(C_4H_4O_6)(C_4H_5O_6)(H_2O)]$, has been carried using X-ray powder diffraction data. Although the presence of praseodymium atom might suggest the use of traditional methods for structure solution, a highly dominant scatterer like praseodymium can often mask the information in the diffraction data concerning the organic component, and consequently the structure completion via traditional methods may be difficult. In the present example, the unit cell obtained from indexing was consistent with the asymmetric unit comprising of two tartrate groups and one praseodymium atom. The structure solution has been carried out in direct space using the program FOX[65]. The tartrate molecular geometry input to the program was fully optimized by an energy gradient method using the program package MOPAC 5.0[77]. Soft constraints on bond distances and bond angles were applied during the Rietveld refinement with GSAS[39]; the tartrate groups were treated as rigid bodies. The final Rietveld plot is shown in Fig. 4.

The structure analysis[78] indicates a 9-fold coordination of Pr atom in respect to oxygen atoms with the metal center displaying a distorted monocapped square antiprism geometry. The molecular structure of the complex reveals infinite parallel chains interlinked through α-hydroxyl oxygen atoms to form a two-dimensional polymeric network. The supramolecular architecture in the complex can be visualized in terms of a planar tetranuclear rectangular unit with a 22-membered $Pr_4C_{10}O_8$ motif (Fig. 5b) having 7.6×6.9 Å dimension. The rectangular building blocks are assembled into helical chains with a period of 21.9 Å running along the *a*-axis (Fig. 5c). The carboxylate groups of tartrate ligands interlink the helical chains to form a three-dimensional polymeric framework (Fig. 5d). To the best of our knowledge, the present one is the second example of a three-dimensional polymeric Pr(III) system and the first report in which the molecular structure of a multidimensional lanthanide tartrate complex has been established from X-ray powder diffraction data.

5.2. *Supramolecular architecture in a binuclear oxo-vanadium (V) – Schiff base complex*

Vanadium (V) complexes capable of binding and cleaving DNA under physiological conditions are of considerable current interest for their potential utility as diagnostic agents in medical science and their model character in relation to active sites of vanadoenzymes. For a better understanding of the structure-activity correlation, knowledge of crystal structure of the model system is essential. In this context, structure

Figure 16: An ORTEP diagram of $C_{23}H_{19}N_3O_6S$ with atom numbering scheme.

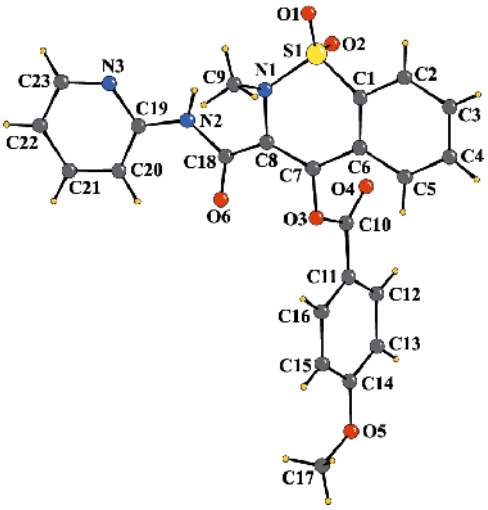

analysis of the binuclear oxo-vanadium (V) complex, $[(VO_2L)_2]$, L=N, N-dimethylenediamine (o-hydroxyl acetophenon), which efficiently binds to DNA and shows photoinduced DNA cleavage activity, was undertaken.

The results of indexing using NTREOR[79] indicated a monoclinic unit cell with FOM values, $M_{25} = 24.0$, $F_{25} = 60.0$ (0.008, 55), and all lines in the powder diffraction pattern indexed. The crystal structure has been determined using a combined reciprocal space-direct space approach and refined by the Rietveld method with GSAS[39]. Full pattern decomposition was performed with EXPO-2004[42] according to Le Bail algorithm using a split type pseudo-Voigt peak profile function and the space group P2/m (the Laue symmetry of the monoclinic system). With 1078 extracted intensities from the powder pattern, a direct method run using EXPO-2004[42] was able to locate the vanadium atom position. Although successive difference Fourier syntheses could build a model structure, the bond distances and angles involving the lighter atoms (C, N, O) deviated significantly from their expected values. To improve the quality of the model structure, the atomic coordinates obtained from the direct method were utilized as input for optimization in direct space using the program FOX[65] implementing the simulated annealing procedure (in parallel tempering mode). The final Rietveld refinement resulted in excellent agreement between observed and calculated powder patterns (Fig. 6). The molecular view of compound is shown in Fig. 7.

The results of structure analysis indicate that the dinuclear complex consists of two edge-sharing vanadium octahedra with each metal center coordinated to one oxo-, one phenolate-, two bridging-oxygen ligands, and two nitrogen donor atoms. The molecular structure reveals a two-dimensional sheet of hexanuclear $R_4^4(24)$ rings (Fig. 8) of dimension 9.0 × 13.9 Å in the *bc*-plane which are further linked through one-dimensional polymeric chains along the [100] direction, and so generating a novel three-dimensional supramolecular architecture. On the basis of structural and photoinduced DNA cleavage studies[80] it is proposed that the dinuclear vanadium complex disintegrates on UV irradiation into two mononuclear species with essentially planar salicylidenemino group so as to fit between the two consecutive base pairs of DNA.

5.3. *Molecular structures of two o-hydroxyacetophenone compounds*

Acetophenone derivatives are probably the most studied organic substrates used for enantioselective bioreduction to the corresponding alcohols. This reduction is mediated by whole cells of a variety of microorganisms. Starting with the products of enantioselective bioreductions of acetophenone derivatives, a wide range of optically active compounds can be synthesized. A knowledge of crystal structure of the starting acetophenone derivative is thus useful for designing subsequent reaction strategies leading to the desired end product with both a high degree of purity and good yield. The present example describes the crystal and molecular structure determination of two o-hydroxyacetophenone derivatives, 1-(2-hydroxy-5-methoxy-4-methylphenyl) ethanone (I) and 1-(2-benzyloxy-5-methoxy-4-methylphenyl) ethanone (II), from laboratory X-ray powder diffraction data.

Indexing of powder patterns for both hydroxy acetophenone derivatives performed with NTREOR[79] showed monoclinic unit cells with volumes compatible to accommodate four molecules. Since the compounds contained only light atoms (C, H, O), the available options for structure solution were limited to the direct methods or global optimization of molecular fragments in direct space. Initial attempts to solve the structures with direct methods using the program EXPO-2004[42] were not successful. It is worth mentioning that the interpretation of electron density map leading to a chemically meaningful model is an important step for successful application of direct methods in solving unknown crystal structures, and the model structure becomes often unrecognizable in the absence of few key atoms. The structures

of both compounds were finally solved in space group P $2_1/c$ via direct space approach using the program FOX[65]. The initial molecular geometries input to FOX were optimized a priori by the energy minimization technique as incorporated in the program package MOPAC 5.0[77], which included the AM1 Hamiltonian. For both compounds the atomic coordinates obtained from the simulated annealing procedure of FOX were taken as the starting models for Rietveld refinement with the program GSAS[39]; the phenyl rings were treated as rigid bodies. The agreement between observed and calculated powder patterns for both compounds (Figs 10 and 12) after Rietveld refinement is remarkably good.

The molecular views of compounds (I) and (II), with atom numbering scheme, are shown in Figs. 9 and 11, respectively. As expected, the molecules of (I) are essentially planar except the methoxy carbon and oxygen atoms (C9, O2), whereas in (II), the two planar fragments (C1–C6, C8–C13) of the molecule are rotated about the C(ph)–O–C–C(ph) linkage by 54.7(1)°. The crystal packing in compounds (I) and (II) exhibits different types of intermolecular hydrogen bonding. The screw related molecules in (I) are connected by C5–H5…O1 hydrogen bond to generate a C(4) chain running along the crystallographic *b*-axis (Fig. 13). In (II), however, C–H…π(arene) hydrogen bonds between the molecules related by the glide plane form an infinite polymeric chain parallel to the [001] direction (Fig. 14).

Figure 17: Formation of two-dimensional sheet of parallel chains running in the [-211] direction for $C_{23}H_{19}N_3O_6S$.

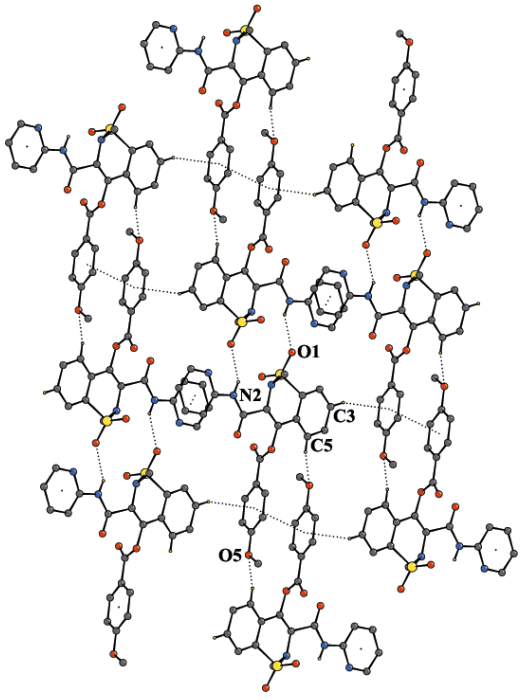

5.4. *Pharmaceutical material*

Knowledge of crystal structures of pharmaceutical materials, which are usually administered in the form of polycrystalline powders, is crucial for a proper understanding and optimizing their biological activity. Piroxicam, 4-hydroxy-2-methyl-N-(2-pyridal)-2H-1,2-benzothiazine-3-carboxamide-1,1-dioxide, and its acyl derivatives are effective non-steroidal anti-inflammatory and analgesic drug against various arthritic and post-operative conditions. Synthesis and structural characterization of different polymorphs of piroxicam related drugs have become an active area of research activity in pharmaceutical industry. In this context, the structure analysis of the piroxicam methoxybenzoate, $C_{23}H_{19}N_3O_6S$, prepared as microcrystalline powder has been undertaken.

Although the indexing and space group assignment from the experimental powder diffraction data of piroxicam derivative have been carried out with the programs TREOR[15] and EXPO-2004[42] without much difficulty, the structure solution part was not straightforward. Attempts to solve the structure by direct methods were not successful due to conformational flexibility of substituted side chains. The structure was finally solved by global optimization of a structural model in direct space using FOX[65]. The molecular geometry used as input in the direct-space structure solution program FOX (operating in parallel tempering mode) was optimized a priori by the energy minimization procedure incorporated in MOPAC 5.0[77]. Bond distances and bond angles were constrained, but torsion angles defining the side chain conformations were allowed to change. During Rietveld refinement, the planar phenyl and pyridine rings were treated as rigid bodies. The final Rietveld plot and molecular view of compound are shown in Fig. 15 and 16, respectively.

The molecular conformation of the compound, as established by the present analysis[81], is similar to that of β-piroxicam polymorph with the anilide oxygen atom (O6) and methoxybenzoyl group lying on the same side of the molecule. A combination of N–H…O, C–H…O and C–H…π(arene) hydrogen bonds, and π…π stacking interactions stabilized the crystal packing. Pairs of intermolecular N–H…O and C–H…O hydrogen bonds join the molecules into centrosymmetric dimers with formation of $R_2^2(14)$ and $R_2^2(22)$ rings which are alternately linked to form an

infinite one-dimensional polymeric chain along the [−211] direction. Interlinking between adjacent chains through C–H...π(arene) hydrogen bonds generates two-dimensional molecular sheets parallel to the (102) plane (Fig. 17), which are further connected via hydrogen bonds to complete the three-dimensional network.

6. Conclusions

The techniques and methods presented here have demonstrated the feasibility of solving crystal structures from laboratory X-ray powder diffraction data and have illustrated the scope and limitations of the methods that are currently available. It is nevertheless important to emphasize that the process of structure determination from powder diffraction data is not a black-box technique, and considerable care must be taken in every stage, i.e. from data collection to final structure refinement, to ensure the correctness of the derived structure model. Continuous advances in the capabilities and efficiencies of techniques used during different stages of structure-determination procedure, coupled with improved data-collection strategies and the speed of computers for data analysis promise an optimistic outlook for the field of crystal structure determination from X-ray powder diffraction data. The future development of indexing methodologies, space group assignment algorithms and optimization techniques will extend the application of powder diffraction in revealing new insights into structural properties of a wide range of materials including important biological systems, such as proteins, for which structural characterization by single-crystal X-ray diffraction technique is not possible.

7. Acknowledgement

The author is grateful to Prof. M. Mukherjee, Dr. S. Mondal, Mr. S. Chakraborty, Mr. S. Ghosh for many useful discussions in connection with the field of research described in this article. Financial support from the University Grants Commission, New Delhi, and the Department of Science and Technology. Govt. of India, through DRS (SAP-I) and FIST programs to Dept. of Physics, Jadavpur University, Kolkata, for purchasing the X-ray powder diffractometer is gratefully acknowledged.

Received 15 July 2007; revised 02 August 2007.

References

1. Harris, K. D. M., Tremayne, M.& Kariuki, B. M. (2001). Angew. Chem. Int. Ed. **40**, 1626.
2. Langford, J. I. & Louer, D. (1996). Rep. Progr. Phys. **59**, 131.
3. David, W. I. F., Shankland, K., McCusker, L. B. & Baerlocher, C. in Structure determination from Powder diffraction data. Oxford University Press. Inc., New York, 2002.
4. Pecharsky, V. K. & Zavalij, P. Y. in Fundamentals of powder diffractions and structural characterization of materials. Spinger Science & Business Media, Inc. USA, 2005.
5. Harris, K. D. M. & Tremayne, M. (1996). Chem. Matter. **8**, 2254.
6. Shankland, K., Markvardsen, A. J. & David, W. I. F. (2004). Z. Kristallogr. **219**, 857.
7. Harris, K. D. M. & Cheung, E. Y. (2004). Chem. Soc. Rev. **33**, 526.
8. Rietveld, H. M. (1969). J. Appl. Crystallogr. **2**, 65.
9. Young R. A. (Editor), The Rietveld Method, International Union of Crystallography, Oxford, 1993.
10. Werner, P. –E. (1992). NIST Spec. Pub. **846**, 503.
11. Baerlocher, C. & McCusker L. B. (1994). Stud. Surf. Sci. Catal. **85**, 391.
12. Louer, D. & Langford, J. I. (1988). J. Appl. Crystallogr. **21**, 430.
13. Azaroff, L. V. & Buerger, M. J. in The powder method in X-ray crystallography, McGraw-Hill, New York, 1980.
14. de-Wolff, P. M. (1957) Acta. Crystallographica. **10**, 590.
15. Werner, P. –E., Eriksson, L. & West Dahl, M. (1985). J. Appl. Crystallogr. **18**, 367.
16. Louer, D. & Louer, M. (1972). J. Appl. Crystallogr. **5**, 271.
17. Visser, J. W. (1969) J. Appl. Crystallogr. **18**, 367.
18. Boultif, A. & Louer, D. (1991). J. Appl. Crystallogr. **24**, 987.
19. Shirley, R. A. CRYSFIRE, Suit of programs for indexing powder diffraction patterns University of Surrey.
20. Neumann, M. A. (2003). J. Appl. Crystallogr. **36**, 356.
21. Kariuki, B. M., Belmonti, S. A. MacMohan, M. I. Johnston, R. L., Harris, K. D. M. & Nelmes, R. J. (1999). J. Synchrotron Radiat. **6**, 87.
22. Nash, J. C. 1990 Compact numerical methods for computers, Bristol: Adam Hilger.
23. Coelho, A. A. (2003). J. Appl. Crystallogr. **36**, 86.
24. de Wolff, P. M. (1968). J. Appl. Crystallogr. **1**, 108.
25. Smith, G. S. & Snyder, R. L. (1979). J. Appl. Crystallogr. **12**, 60.
26. Shirley, R. (1980). NBS Spec. Pub. No. **567**, 361.
27. Werner, P. –E. (1980). NBS Spec. Pub. No. **567**, 503.
28. Toraya, H. (1986). J. Appl. Crystallogr. **19**, 440.
29. Zhukov, S. G., Chernyshev, V. V., Babaev, E. V., Sonneveld, E. J. & Schenk H. (2001), Z. Kristallogr. **216**, 5.
30. Pawley, G. S. (1981) J. Appl. Crystallogr. **14**, 357.
31. Le Bail, A., Duroy, H. & Fourquet, J. L. (1988). Mater. Res. Bull. **23**, 447.
32. Jansen, I., Peshar, R. & Schenk, H. (1992). J. Appl. Crystallogr. **25**, 231.
33. Sivia, D. S. & David, W. I. F. (1994). Acta Cryst. **A50**, 703.
34. Altomare, A., Burla, M. C., Camalli, M., Carrozzini, B. Cascarano, G. Giacavazzo, C. Gaugliardi, A. Moliterni, A. G. G., Polidori, G. & Rizzi, R. (1999). J. Appl. Crystallogr. **32**, 339.
35. Altomare, A., Giacovazzo, C., Moliterni, A. G. G. & Rizzi, R. (2001). J. Appl. Crystallogr. **34**, 704.
36. Carrozzini, B., Giacovazzo, C., Gaugliardi, A., Rizzi, R. Burla, M. C. & Polidori, G. (1997). J. Appl. Crystallogr. **30**, 92.
37. Pawley, G. S. (1981). J. Appl. Crystallogr. **14**, 357.
38. Toroya, H. (1986). J. Appl. Crystallogr. **19**, 440.
39. Le Bail, A., Duroy, H. & Fourquet, J. L. (1988). Matter. Res. Bull. **23**, 447.
40. Rodriguez-Carvajal, J. In collected abstracts of powder diffraction meeting: Toulouse, France, July, 1990: p. 127.
41. Cock Croft, J. K. PROFIL, Version 5.17, Department of Crystallography, Brikbeck College, U.K., 1994.
42. Altomare, A., Caliandro, R., Camalli, M., Coucci, C., Giacovazzo, C., Moliterni, A. G. G. & Rizzi, R. (2004) J. Appl. Crystallogr. **37**, 1025.
43. Markvardsen, A. J., David, W. I. F. & Shankland, K. (2002). Acta Cryst. **A58**, 316.
44. Altomare, A., Coucci, C., Giacovazzo, C., Moliterni, A. G. G. & Rizzi, R. (2006). J. Appl. Crystallogr. **39**, 558.
45. Wilson, C. C. & Wadsworth, J. W. (1990). Acta Crystallogr. **A46**, 258.
46. Rius, J. & Miravitlles, C. (1988). J. Appl. Crystallogr. **21**, 224.
47. Cirujeda, J., Ochando, L. E., Amigo, J. N., Rovira, C., Rius, J. & Veciana, J. (1995). Angew. Chem., Int. Ed. Enlg., **34**, 55.
48. Main, P. MULTAN84, University of York, U. K. 1984.
49. Sheldrick, G. M.: SHELXL97 and SHELXS97. Crystal structure solution and refinement program. University of Göttingen, Germany. (1997).
50. Burla, M. C., Camalli, M., Cascarano, G., Giacovazzo, C., Polidori, G., Spagna, R. & Viterbo, D. (1989). J. Appl. Crystallogr. **22**, 389.
51. Altomare, A., Cascarano, G., Giacovazzo, C., Gaugliardi, A., Burla, M. C., Polidori, G. & Camalli, M. (1994). J. Appl. Crystallogr. **27**, 435.
52. Cochan, W. (1955). Acta Crystallogr. **8**, 473.
53. Altomare, A., camalli, M., Cuocci, C., Giacovazzo, C., Moliterni, A. G. G. & Rizzi, R. (2007) J. Appl. Crystallogr. **40**, 344.
54. Tremayne, M., Lightfoot, P., Mehta, M. A., Bruce, P. G., Harris, K. D. M., Shankland, K., Gillmore, C. J. & Bricogne, G. (1992) J. Solid. Stare. Chem. **100**, 191.
55. Gillmore, C. J., Henderson, K. & Bricogne, G. (1991). Acta Crystallogr. **A47**, 830.
56. Tremayne, M., Lightfoot, P., Glidewell, C., Harris, K. D. M., Shankland, K., Gillmore, C. J., Bricogne, G. & Bruce, P. G. (1992). J. Matter. Chem. **2**, 1301.
57. Shankland, K., Gillmore, C. J., Brecogni, G. & Hashizume, H. (1993). Acta Crystallogr. **A49**, 493.
58. Gillmore, C. J., Bricogne, G. & Bannistar, C. (1990). Acta Crystallogr. **A46**, 297.
59. Harris, K. D. M. (1999). J. Chim. Chem. Soc. **46**, 23.
60. Freeman, C. M., Gorman, M. & Newsam, J. M. in computer modeling in inorganic crystallography (Ed.: C R A Catlow), Academic Press, San Diego, 1997.
61. Harris, K. D. M., Tremayene, M., Lightfoot, P. & Bruce, P. G. (1994). J. Am. Chem. Soc. **116**, 3543.
62. Hammond, R. B., Roberds, K. J., Docherty, R. & Edmondson, M. (1997). J. Phys. Chem. B. **101**, 6529.
63. Reck, G., Kretshemer, R. G., Kutschabsky, L. & Pritzkow, W. (1988). Acta Cryttalogr. **A44**, 417.
64. Andreeve, Y. G., Lightfoot, P. & Bruce, P. G. (1997). J. Appl. Crystallogr. **30**, 294.
65. Favre-Nicolin, V. and Cerný, R. (2002). J. Appl. Crystallogr. **35**, 734.
66. Angel, G. E., Wilke, S., Konig, O., Harris, K. D. M. & Leusen, F. J. J. (1999). J. Appl. Crystallogr.**32**, 1169.
67. Le Bail, A. (2001). Mater. Sci. Forum, **378-381**, 65.

68. Bruker AXS GmbH (2000). TOPAS, User's Manual.
69. Harris, K. D. M., Johnston, R. L., Albesa Jove, D., Chao, M. H., Cheung, E. Y., Hbershon, S., Kariuki, B. M., Lanning, O. J., Tedesco, E. & Tuner, G. W. EAGER, University of Birmingham. 2001
70. Putz, H., Schen, J. C. & Jansen, M. (1999). J. Appl. Crystallogr. **32**, 864.
71. David, W. I. F., Schankland, K. & Schankland, M. (1998). Chem. Comm. **8**, 931.
72. Kariuki, B. M., Serrano-Gonzales, H., Johnston, R. L. & Harris, K. D. M. (1997). Chem. Phys. Lett. **280**, 189.
73. Keane, A. J. (1996). Modern Heuristic Search Methods, edited by V. Rayward-Smith, I. Osman, C. Reeves & G. D. Smith, pp. 255-272. New York: Wiley.
74. Harris, K. D. M., Johnston. R. L. & Kariuki, B. M. (1998). Acta Crystallogr. **A54**, 632.
75. Shankland, K., David, W. I. F. & Csoka, T. (1997). Z. Kristallogr. **212**, 550.
76. Izumi, F., Asano, H., Murata, H. & Watanabe, N. (1987). J. Appl. Crystallogr. **20**, 411.
77. Stewart, J. J. P. MOPAC, Version 5.0, Quantum Chemistry program exchange581; Indiana University, 1988.
78. Mondal, S., Mukherjee, M., Chakraborty, S. & Mukherjee, A. K. (2006). Cryst. Growth & Des. **6**, 940.
79. Altomare, A., Giacovazzo, C., Gaugliardi, A., Moliterni, A. G. G., Rizzi, R. & Werner, P. -E. (2000). J. Appl. Cystallogr. **33**, 1180.
80. Mondal, S., Mukherjee, M., Dhara, K., Ghosh, S., Ratha, J., Banerjee, P. & Mukherjee, A. K. (2007). Cryst. Growth & Des. (in press).
81. Chakraborty, S., Ghosh, S., Cheemala, J. M. S., Jayaselli, J., Pal, S. & Mukherjee, A. K. (2007). Z. Kristallogr. (in press).

Dr. Alok K. Mukherjee is a graduate of the University of Calcutta (B.Sc., 1969). After Ph.D (Sc) in 1977 from Visva-Bharati University, Santiniketan, he joined National Physical Laboratory, New Delhi. In 1981, he moved to Jadavpur University, Calcutta, where he is currently a Professor in Physics. During 1987–1989 and 1997 he visited University of York and University of Manchester, England, to work with Prof. M. M. Woolfson, F. R. S., Prof. P. Main and Prof. J. R. Helliwell on "Application of Direct methods in macromolecular crystallography". Professor Mukherjee's research covers several areas relating to structural crystallography, structural disorder with some focus at present on the development and application of new techniques for structure determination from laboratory X-ray powder diffraction data, and microstructural characterization of biological materials, for example, bone, teeth, kidney and gall-bladder stones. He has authored about 100 research papers in various international journals.